Computational Study on Flow Control Characteristics of Synthetic Jets over a Blended Wing Body Configuration

Minhee Kim[1)], Byunghyun Lee[2)], and Chongam Kim[2)]

[1)] *Interdisciplinary Program in Computational Science & Technology, Seoul National University, Seoul, KOREA*
[2)] *Department of Aerospace Engineering, Seoul National University, Seoul, KOREA*

Flow control using synthetic jets has been computationally investigated to improve aerodynamic performance of blended wing body configuration under different jet location at a relatively high angle of attack. Experimental and numerical data were examined by analyzing the baseline characteristics of a blended wing body configuration when synthetic jet was off. Based on the aerodynamic data and flow structure, a strategy for flow separation control on the blended wing body configuration was established. Two types of exit locations were considered: one is outboard array jets, and the other is inboard array jets. The interactions of synthetic jets with a free stream were performed by analyzing the vortical structure and the surface pressure characteristics. The effectiveness of flow control was evaluated by examining the aerodynamic coefficient and flow structures. As a result, the vortex breakdown point is moved toward the outboard section by synthetic jets, and the separation flow shows a stable structure. This indicates that the synthetic jets under suitable actuating conditions beneficially change the local flow feature and vortex structure to bring a significant improvement of the wing aerodynamics acting on the blended wing body configuration in the stall angle.

Key Words: Synthetic jet, Flow control, UAV, CFD, BWB

Nomenclature

A_{jet}	: instantaneous peak velocity at orifice
h	: slot width
f	: frequency of periodic excitation
U	: velocity
x	: streamwise distance
y	: spanwise distance from centerline
z	: normal distance from wall

Subscripts

0	: reference value
∞	: freestream value

1. Introduction

Control of flow separation by means of synthetic jets is known to be quite effective in a variety of flow conditions[1)]. Synthetic jets have been widely used in fluid dynamic applications including static and dynamic stall control of airfoils[2-3)], jet vectoring[4)], jet mixing enhancement[5)], and thermal mixing[6)]. There have been numerous studies on the benefits of synthetic jets as a control or mixing device. A synthetic jet periodically transports momentum from a jet cavity to an outside region, thus interacting with an external flow field through a series of jet vortices. Many studies have conducted on the interaction between external cross flows and synthetic jets. Some of them have focused on the formation of a synthetic jet in a turbulent mixing layer, and assessed its behavior under various conditions.

Studies on synthetic jets have been performed by both experimental and numerical methods. Experimental studies have revealed jet characteristics and jet vortex formation. Crook and Wood investigated the behavior of synthetic jets in quiescent conditions, in a cross-flow and in a boundary layer[7)]. They investigated the delay of flow separation on a 2-D circular cylinder by using an array of synthetic jets. Greenblatt *et al.* investigated flow separation control using both a steady suction and a synthetic jet[8-9)]. They experimentally studied the control of a separated flow over a wall-mounted hump to generate a data set for the development and evaluation of computational methods. Surface pressure data under various flow conditions were produced by zero mass flux control, steady suction control, and the baseline case. Amitay and Cannelle studied the evolution and transient behavior of finite span synthetic jets using hot wire anemometry and PIV techniques. They examined the effect of the slot aspect ratio on the development of the synthetic jet, and the spatial evolution of secondary three-dimensional vortical structures in the flow field[10-11)]. Kim *et al.* performed a study on the characteristics of synthetic jets for different exit configurations under various flow conditions[12)]. Through various comparisons, they observed that the exit configuration should be regarded as an important design parameter.

At the same time, a number of numerical studies have also been carried out. Mittal *et al.* examined the

formation and interaction of a synthetic jet with a flat plate boundary layer in a three-dimensional configuration[13]. Rumsey *et al.* performed a study of synthetic jet flows into a turbulent boundary layer crossflow through a circular orifice[14]. Kim and Kim numerically investigated the frequency-dependent flow control mechanisms of synthetic jets on an airfoil, and proposed multi-location synthetic jets to mitigate the unstable flow structures of a high-frequency jet[15]. Subsequently, Kim *et al.* applied synthetic jets to improve the aerodynamic performance of tilt-rotor UAV airfoils in hovering and transition flight modes[16]. Zhong *et al.* examined the vortex structures produced by a synthetic jet in water, and presented the vortex roll-up criterion according to the Stokes length using experimental and numerical methods[17]. In addition, the fluid physics underlying the interaction process between circular synthetic jet and a laminar boundary layer was investigated by 3-D numerical simulations[18].

The focus of the present paper is to study the flow characteristics of synthetic jets at different jet location on a blended wing body configuration. Experimental and numerical data is examined by analyzing the baseline characteristics of a blended wing body configuration when synthetic jet is off. Based on the aerodynamic data and flow structure, a strategy for flow separation control on the blended wing body configuration is established. Synthetic jet actuators are installed to prevent leading-edge stall at high angles of attack. Two types of exit locations were considered: one is outboard array jets, and the other is inboard array jets. The interactions of synthetic jets with a free stream are performed by analyzing the vortical structure characteristics. Numerical results are examined by changing jet location. The effectiveness of flow control was evaluated by examining the aerodynamic coefficient and flow structures.

2. Experimental Reference

An experimental evaluation of the low speed performance of the modified 1303 was carried out by subsonic wind tunnel with a test section of 4 m × 3 m at the KARI (Korea Aerospace Research Institute). The instrumental uncertainty in velocity measurement is found to be less than 0.1 m/s. The configuration has a mean aerodynamic chord of 1.184 m and a span of 2 m. In order to flow control efficiency, the leading-edge sweep angle and twist angle at wing tip is selected as 47 degree and -5 degree.

Synthetic jet actuators (7 modules on each wing) were installed to prevent leading-edge stall at high angles of attack. The exit configuration of actuator was circular exit, which has 17 circular holes of a hole diameter of 1.5 mm, a hole gap of 1.5 mm. The Reynolds number of the mean chord length is 9.6×10^5, the free stream velocity is 20 m/s, the jet frequency is fixed at 200 Hz, and the maximum velocity of the synthetic jet is 40 m/s.

Static pressure taps were installed on the different wing sections. Static pressure was obtained using a net pressure scanner. Forces and moments were acquired via an external six-component balance.

Fig. 1 BWB configuration installed wind tunnel at the KARI

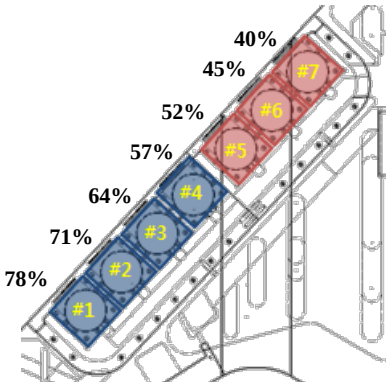

Fig. 2 Synthetic jet location along the spanwise direction

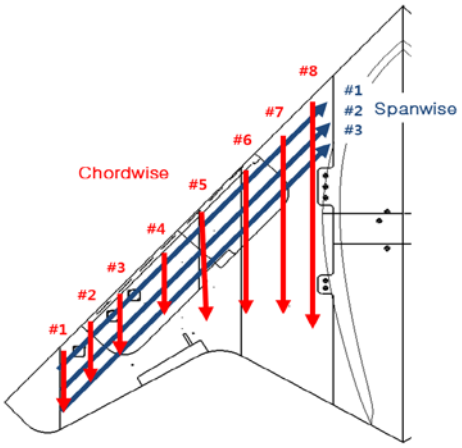

Fig. 3 Locations of pressure tabs

3. Numerical Methods

3.1. Governing Equations

Accurate prediction of stall characteristics with or without turbulence models is still an extremely challenging task. By considering available computing power and required numerical accuracy, the present approach relies on solving Unsteady Reynolds-averaged Navier-Stokes (URANS) equations. URANS simulation combined with adequate turbulence models, such as the κ-ω SST turbulence model, can provide reasonably good solutions[19].

The incompressible governing equations are given by the continuity equation and the momentum equation for the conservation of mass and momentum, where the over-bar indicates a Reynolds-averaged quantity.

$$\nabla \cdot \bar{u} = 0 \tag{1}$$

$$\rho \frac{\partial \bar{u}}{\partial t} + \rho \bar{u} \cdot \nabla \bar{u} = -\nabla \bar{p} + (\mu + \mu_t) \nabla^2 \bar{u} \tag{2}$$

The governing equations were then solved in a time-accurate manner by employing the method of pseudo-compressibility, where τ is the pseudo-time and β is the pseudo compressibility parameter[20-21].

$$\frac{\partial \bar{p}}{\partial \tau} = -\beta \nabla \cdot \bar{u} \tag{3}$$

The upwind differencing scheme based on flux-difference splitting, combined with the MUSCL approach, was used to calculate the convective term with a third-order spatial accuracy. The viscous fluxes were then centrally differenced by a second-order spatial accuracy, and the flow variables were updated by the LU-SGS time integration[22]. The turbulence model used in the present computation is the Menter's shear stress transport two-equation model, which has provided excellent predictions of flows involving separation[21,23]. Also, Total Stress Limitation (TSL) method was employed to include the effect of flow transition[24]. All computations were performed with a finite volume-based in-house code that had been extensively validated[14,15,21].

3.2. Synthetic jet Boundary Conditions

A synthetic jet actuator is an oscillatory jet generator that requires zero-net mass input yet produces a non-zero momentum output. Figure 4 shows a schematic of a synthetic jet actuator that contains an enclosed cavity with a small orifice on one face. At CFDVAL2004, Rumsey *et al.* reported that, compared to experiment data, the velocity distributions near the orifice exit might exhibit some anomalies neither captured nor modeled by CFD, but they also mentioned that global flow features could be captured with a reasonably good accuracy[15,16,19,25].

Based on these results, the suction/blowing-type boundary condition proposed by Kral *et al.*, as in Eq. (4), was applied to the synthetic jet actuator[26]. The 'top hat' condition, wherein the spatial variation of the jet at the orifice was neglected, was employed to obtain computationally efficient results without compromising physical reality[27]. A perturbation to the flow-field was then introduced by the jet velocity where ξ denotes the streamwise direction, η denotes the spanwise direction, ζ denotes normal direction from the wall, $\vec{u}_n$ is a velocity vector, and $\vec{d}_{jet}$ is a unit vector in the jet direction. Spatial variation over the orifice was neglected, and assumed as a top hat distribution.

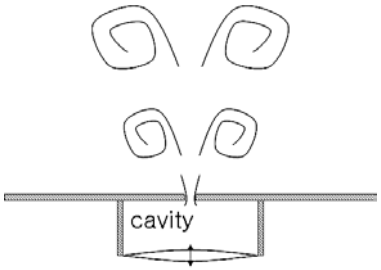

Fig. 4 Schematic of a synthetic jet

4. Results and Analysis

4.1. Control-off case

Verification study has been performed in term of grid refinement. To examine the grid sensitivity, three grid densities were considered for the control-off case. From the comparison of the computed results depicted in Fig. 5, computational differences between fine mesh and medium mesh are less than 2%, which is thought to be adequate for reliable computations. Thus, mesh systems of 6.1 million grid points was considered for the control-off case.

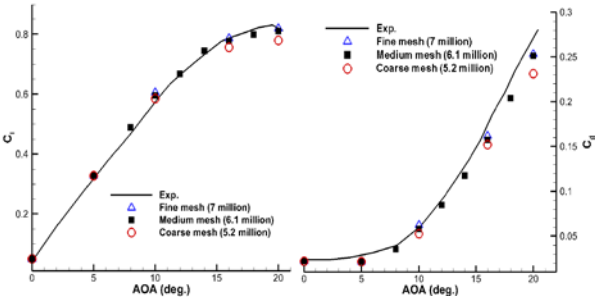

Fig. 5 Lift and drag coefficient curves (control-off case)

Flow feature comparisons are shown in the next series of pictures in Fig. 6a-d and Fig. 7a-d. Figure 6 shows areas of flow separation plotted on top of the pressure coefficient C_P contours over the wing surface for the

angle of attack ranging from 8 degree to 14 degree. At angle of attack of 8 degree (Fig. 6a), the suction area appears along the leading-edge, which means that the leading-edge vortex is developed on the surface. At the angle of attack of 10 degree (Fig. 6b), the leading-edge vortex expand toward trailing-edge and the small separation flow is observed near the wing tip of the wing. At angles of attack of 12 degree and 14 degree (Fig.6c-d), the vortex breakdown is shown at the midboard section of the wing and a large separation region appears on the outboard section. As a result, the vortex breakdown region and separated-flow region are merged into each other, and the multiple patterns of separation present on the wing suction surface. As the angle of attack increases, the size of the suction area developed from the leading-edge becomes larger and the separated flows expand from the outboard section to the inboard section.

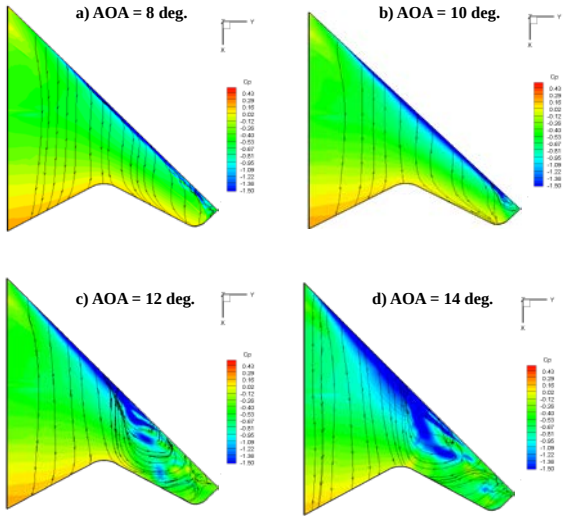

Fig. 6 Surface pressure coefficient contour (control-off case)

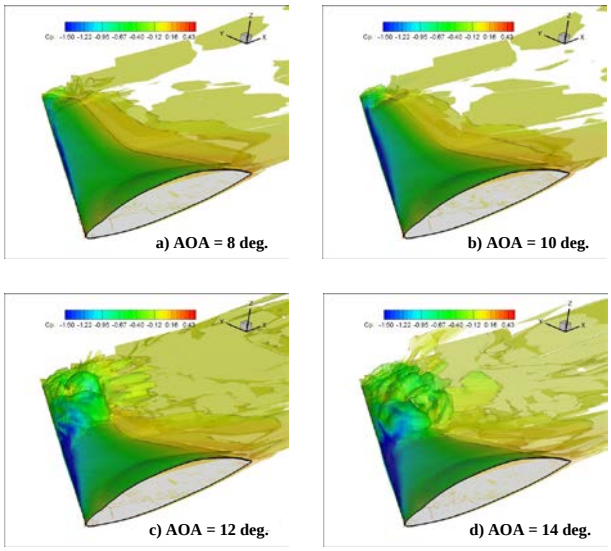

Fig. 7 Iso-vorticity contour colored pressure coefficient (control-off case)

Figure 7 shows iso-vorticity contour colored pressure coefficient. The vorticity contours present the tendency of flow structure as increase of angle of attack. The leading-edge vortex develops from the aft of leading edge and flow separation starts from outboard of wing. Through an analysis of computed flowfields, it is observed that both the vortex breakdown in the inboard section and the separation in the outboard section are critical in determining the aerodynamic performance. Thus, the leading-edge vortex breakdown and flow separation controls are carried out to improve the aerodynamic performance of the wing.

4.2. Control-on case

For the control of leading-edge vortex flow and the improvement of the local lift-to-drag, synthetic jet actuators was installed at the leading edge along the spanwise direction from 40 % span to 78 % span. To find the effective flow control method according to the position of leading-edge vortex breakdown, flow control experiments were performed by changing the number of synthetic jet modules at the α = 12 degree. In the results of experimental analysis, synthetic jets located inboard section and outboard section have an effective flow control performance similarly. In order to analyze the flow mechanism, numerical simulation was conducted according to the position of synthetic jet modules. Figure 8 shows synthetic jet modules performed flow analysis using numerical simulation. Case 1 is the jet modules located in outboard section (#1, #2) and case 2 is the jet modules located in inboard section (#6, #7).

Figure 9 compares numerical results with experimental data on three levels of grid density for each case. The computed results show a reasonable agreement with experimental data. Thus, mesh systems of 17 million grid points were considered for the both cases. The numerical simulation is believed to be fully capable of simulating the behavior of synthetic jets for the flow control over a blended wing body configuration.

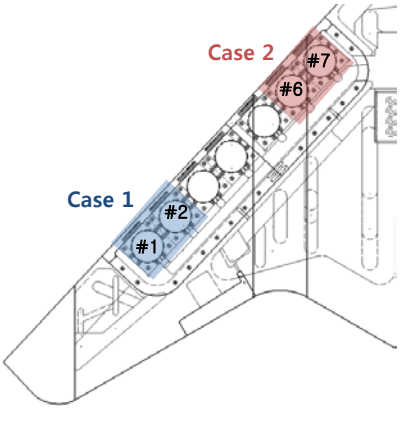

Fig. 8 Synthetic jet actuation type

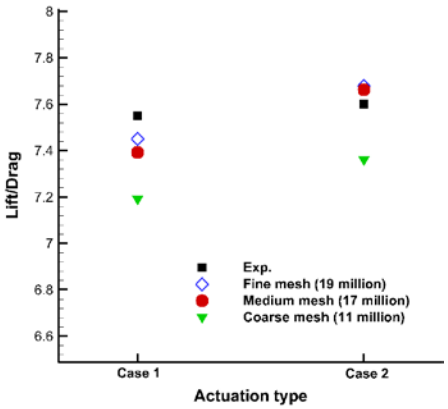

Fig. 9 Lift to drag coefficients (control-on case)

Figure 10 presents the results of the phase-averaged surface pressure coefficient for the control-off and control-on cases. In the case of outboard jet (case 1), synthetic jets are located in the separated-flow region. Synthetic jets control the outboard flow feature and reduce the separation region. For the inboard jet (case 2), synthetic jets are near the position of leading-edge vortex breakdown. The vortex breakdown point is moved toward the outboard section by synthetic jets, and the separation flow shows a stable structure.

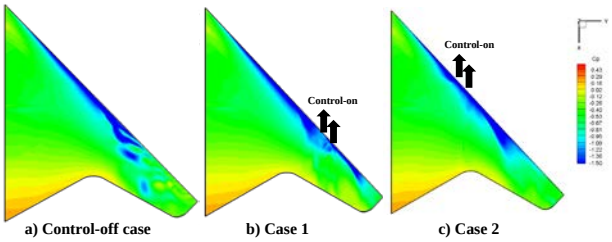

Fig. 10 Phase-averaged surface Cp contour (control-on case)

The evolution of a jet vortex formation provides insight on the interaction between the free stream and the synthetic jet. Figures 11 and 12 show iso-surface vorticity colored pressure coefficient and velocity magnitude of the two cases. The outboard synthetic jets suppress the formation of the flow separation. The vortices produced by the outboard jet continuously disturb the large separation vortex, leading to the substantial reduction of separation flow. As shown in Fig. 12, the synthetic jets located in inboard section positively interfere with the leading-edge vortex breakdown. The flow near the synthetic jet slot is firmly attached, and as a result, a more stable flow structure is developed on the suction surface.

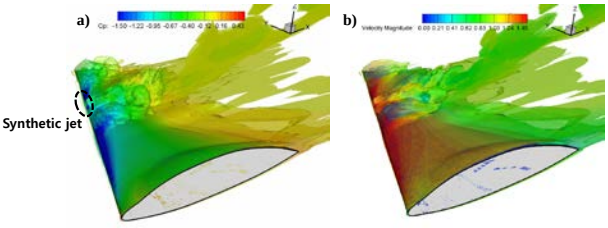

Fig. 111 Phase-averaged iso-vorticity contours (case 1)
a) : colored Cp, b) : colored velocity magnitude

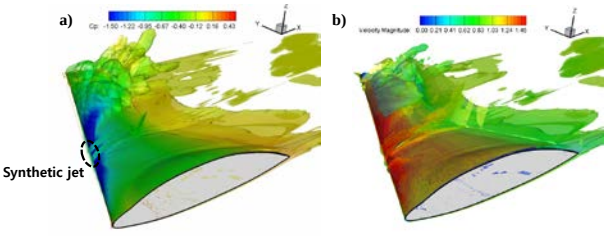

Fig. 122 Phase-averaged iso-vorticity contours (case 2)
a) : colored Cp, b) : colored velocity magnitude

Figures 13 and 14 are phase-averaged pressure coefficient contour along the spanwise direction for each case. Compared to control-off case, significant role of synthetic jets according to the jet location is observed again. In the case of jets in the outboard section (case 1), the size of the leading-edge separation vortex substantially decreases at 80-90 percent of span length. For the inboard jets (case 2), the starting point of vortex breakdown is moved toward outboard section from 65 percent of span to 75 percent of span.

Through the analyses on the flow control performance, it is observed that synthetic jet under suitable actuating conditions beneficially changes the local flow feature and vortex structure to bring a significant improvement of the wing aerodynamics acting on the blended wing body configuration in the stall angle.

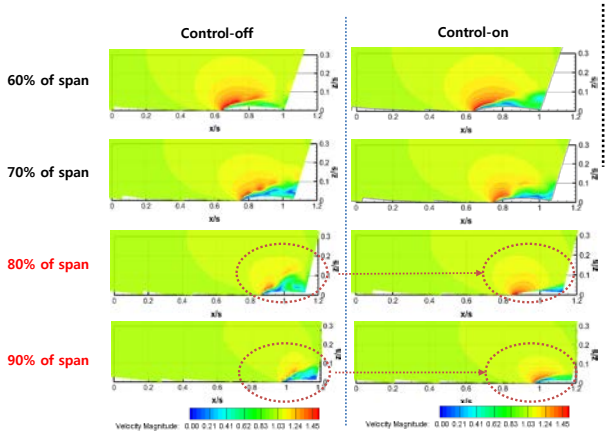

Fig. 133 Phase-averaged Cp contour along the spanwise direction
(case 1)

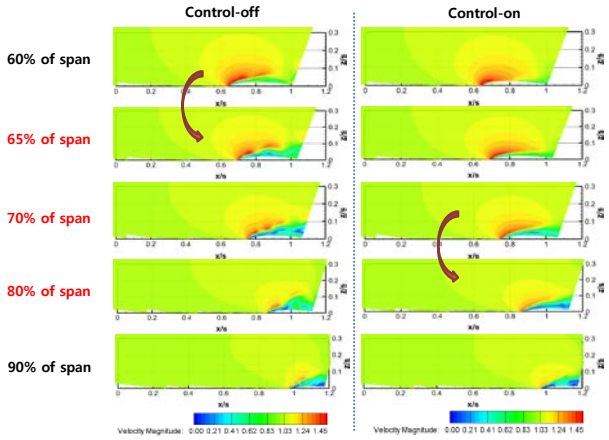

Fig. 144 Phase-averaged Cp contour along the spanwise direction
(case 2)

5. Conclusions

Flow control on a blended wing body configuration using synthetic jets was numerically investigated for different jet location at a relatively high angle of attack. The synthetic jet was able to control leading-edge vortex breakdown and flow separation, thus change the global flow-field structure favorably. Consequently, stall characteristics and control surface performance were remarkably improved.

Experimental and numerical data were examined by analyzing the baseline characteristics of a blended wing body configuration when synthetic jet was off. Based on the aerodynamic data and flow structure, a strategy for flow separation control on the blended wing body configuration was established. Synthetic jet actuators were installed to prevent leading-edge stall at high angles of attack. Two types of exit locations were considered: one is outboard array jets, and the other is inboard array jets. Numerical results were examined by changing jet location. The interactions of synthetic jets with a free stream were performed by analyzing the vortical structure and the surface pressure characteristics. The effectiveness of flow control was evaluated by examining the aerodynamic coefficient and flow structures. As a result, the vortex breakdown point is moved toward the outboard section by synthetic jets, and the separation flow shows a stable structure.

Based on the numerical results and comparisons, it is observed that the synthetic jet under suitable actuating conditions beneficially changes the local flow feature and vortex structure to bring a significant improvement of the wing aerodynamics acting on the blended wing body configuration in the stall angle.

Acknowledgments

Authors gratefully acknowledge the financial supports of the Defense Acquisition Program Administration and Agency for Defense Development (UC100031JD), and KISTI Supercomputing Center (KSC-2012-C3-38).

References

1) D. Greenblatt, I. Wygnanski, “Control of Separation by Periodic Excitation”, *Progress in Aerospace Science*, Vol. 37, No. 7, 2000, pp. 487-545.
2) M. Amitay, D. R. Smith, V. Kibens, D. E. Parekh, A. Glezer, “Aerodynamic Flow Control over an Unconventional Airfoil using Synthetic Jet Actuators”, *AIAA Journal*, Vol. 39, No. 3, 2001, pp. 361-370.
3) L. W. Traub, A. Miller, O. Rediniotis, “Effects of Synthetic Jet Actuation on a Ramping NACA 0015 airfoil”, *Journal of Aircraft*, Vol. 41, No. 5, 2004, pp. 1153-1162.
4) B. L. Smith, A. Glezer, “Jet Vectoring using Synthetic Jets”, *Journal of Fluid Mechanics*, Vol. 458, 2002, pp. 1-34.
5) H. Wang, S. Menon, “Fuel-Air Mixing Enhancement by Synthetic Microjets”, *AIAA Journal*, Vol. 39, No. 12, 2001, pp. 2308-2319.
6) A. Pavlova, M. Amitay, “Electronic Cooling Using Synthetic Jet Impingement”, *Journal of Heat Transfer*, Vol. 128, Sep. 2006, pp. 897-907.
7) A. Crook, N. J. Woodf, “Measurements and Visualizations of Synthetic Jets”, *39th Aerospace Sciences Meeting and Exhibit*, AIAA 2001-0145, Reno, Nevada, 8-11 January 2001
8) D. Greenblatt, K. B. Paschal, C. S. Yao, J. Harris, “Experimental Investigation of Separation Control, Part 1: Baseline and Steady Suction”, *AIAA Journal*, Vol.44, No. 12, Dec. 2006, pp. 2820-2830.
9) D. Greenblatt, K. B. Paschal, C. S. Yao, J. Harris, “Experimental Investigation of Separation Control, Part 2: Zero mass-flux Oscillatory Blowing”, *AIAA Journal*, Vol.44, No. 12, Dec. 2006, pp. 2831-2845.
10) F. Cannelle, M. Amitay, “Transitory Behavior of a Finite Span Synthetic Jet”, *Physics of Fluids*, Vol. 19, Issue 9, 2007.
11) M. Amitay, F. Cannelle, “Evolution of Finite Span Synthetic Jets”, *Physics of Fluids*, Vol. 18, Issue 5, 2006.
12) W. Kim, C. Kim, K. J. Jung, “Separation Control Characteristics of Synthetic Jets Depending on Exit Configuration”, *AIAA Journal*, Vol. 50, No. 3, 2012
13) B.R.Ravi, R. Mittal, F.M. Najjar, “Study of Three-Dimensional Synthetic Jet Flowfields Using Direct Numerical Simularion”, AIAA 2004-0091, *42nd AIAA Aerospace Sciences Meeting and Exhibit*, Reno, NV, 5-8 January, 2004
14) C.L. Rumsey, N.W. Schaeffler, I.M. Milanovic, K.B.M.Q. Zaman, “Time-Accurate Computations of Isolated Circular Synthetic Jets in Cross flow”,

Computers & Fluids, Vol. 36, Issue 6, July 2007, pp. 1092-1105

15) S. H. Kim, C. Kim, "Separation Control on NACA23012 using Synthetic Jet", *Aerospace Science and Technology*, Vol. 12, No. 4-5, 2009, pp. 172-182.

16) M. Kim, S. H. Kim, W. Kim, Y. Kim, C. Kim, "Flow Control of Tilt-Rotor Airfoils using Synthetic Jets", *Journal of Aircraft*, Vol. 48, No. 3, May–June 2011, pp. 1045-1057

17) S. Zhang, S. Zhong, "Experimental Investigation of Flow Separation Control Using an Array of Synthetic Jets", *AIAA Journal*, Vol. 48, No. 3, Mar. 2010, pp. 611-623.

18) J. Zhou, S. Zhong, "Numerical Simulation of the Interaction of a Circular Synthetic jet with a Boundary Layer", *Computers & Fluids*, Vol. 38, No. 2, 2009, pp. 393-405.

19) C.L. Rumsey, T.B. Gatski, W.L. Seller III, V.N. Vasta, S.A. Viken, "Summary of the 2004 CFD validation workshop on synthetic jets and turbulent separation control", *2nd AIAA Flow Control Conference*, AIAA-2004-2217, Portland, Oregon, June 28-1, 2004.

20) Chorin, A. J., "A Numerical Method for Solving Incompressible Viscous Flow Problems", *Journal of Computational Physics*, Vol. 2, Issue 1, August 1967, pp.12-26.

21) Kim, C. S., Kim, C., Rho, O. H., "Parallel Computations of High-Lift Airfoil Flows Using Two-Equation Turbulence Models", *AIAA Journal*, Vol. 38, No. 8, 2000, pp. 1360-1368.

22) Yoon, S., Kwak, D., "Three-Dimensional Incompressible Navier-Stokes Solver Using Lower-Upper Symmetric Gauss Seidel Algorithm", *AIAA Journal*, Vol. 29, No. 6, 1991, pp. 874-875.

23) J.E. Bardina, P.G. Huang, T.J. Coakley, "Turbulence modeling validation, testing and development", *NASA TM-110446*, April 1997.